1 mm^3 Resolution Breast-Dedicated PET System

Frances W. Y. Lau, Chen Fang, Paul D. Reynolds, Peter D. Olcott Arne Vandenbroucke, Virginia C. Spanoudaki, Femi Olutade, Mark A. Horowitz, and Craig S. Levin

***Abstract* – We are developing a 1 mm^3 resolution breast-dedicated Positron Emission Tomography (PET) system in an effort to increase the role of PET in earlier stages of breast cancer management. The system consists of two 16 cm x 9 cm x 2 cm detector panels constructed using stacked layers of 8x8 arrays of 1 mm^3 LSO scintillation crystals coupled to Position Sensitive Avalanche Photodiodes (PSAPDs). Preliminary detector characterization indicates that analog multiplexed PSAPD signals coupled to ASIC readout electronics are able to resolve the 8x8 arrays of LSO crystals with an average peak-to-valley ratio of about 14, an energy resolution of 14.4% ± 0.8% at FWHM for the 511 keV photo-peak, and a paired coincidence photon time resolution of 7.3 ± 0.2 ns FWHM using the ASIC (5.2 ± 0.1 ns FHWM unpaired photon time resolution). Each 1 cm^2 area PSAPD chip under bias generates 2 to 4 mW of power, and thus thermal regulation is required. A finite volume simulation of the detectors with thermal regulation features incorporated in the panels indicates that the maximum temperature variation across the thermally regulated imaging head is 4 degrees Celsius.**

I. Introduction

CURRENTLY, Positron Emission Tomography (PET) does not play a significant role in breast cancer management. Standard clinical PET systems have low photon efficiency geometries, long scan times, and insufficient spatial and contrast resolutions for early breast cancer identification. To address these issues, we are developing a two panel breast-dedicated PET system with 1 mm^3 intrinsic resolution and high photon sensitivity. The system form factor is designed so that the system is portable, and can, for example, be easily transported into operating rooms for use in guiding biopsy or cancer staging, in addition to diagnosis. For biopsy guidance, we will use a radioactive biopsy needle and acquire sequential images to guide the position of the needle.

II. System Design

A. System Geometry and Form Factor

The system consists of two imaging heads, each with a 16 cm x 9 cm x 2 cm detector panel (Fig. 1). The panels are comprised of 4608 Position Sensitive Avalanche Photodiodes (PSAPDs) attached to an 18,432 channel data acquisition system. The system is compact enough to be used during prone needle biopsy and other surgical procedures.

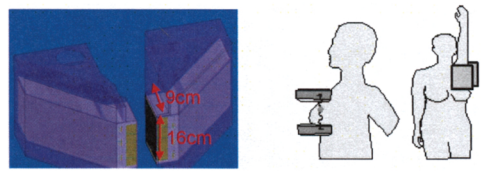

Fig. 1. Left: 9x16 cm^2 imaging heads, including data acquisition. Right: two potential breast imaging orientations.

In contrast to clinical systems that typically only detect about 1% of the photon coincidences, simulations showed that this system captures 8 to 14% of the photons for a panel separation of 4 to 8 cm (energy window is 350-650 keV; time window is 6 ns) [1].

B. High Resolution Detector

The detector is comprised of stacked layers of 8x8 arrays of 1x1x1 mm^3 LSO (lutetium orthosilicate) scintillation crystals coupled to thin PSAPDs. A Dual-LSO-PSAPD module, shown in Fig 2, consists of two LSO arrays, each coupled to a PSAPD mounted on a flex circuit. An alumina frame in the detector module provides mechanical support. The PSAPDs, manufactured by Radiation Monitoring Devices (RMD), Inc. (Watertown, MA), have 8x8mm^2 sensitive area with a gain of about 1000 when biased with 1750V.

As shown in Fig. 3, the Dual-LSO-PSAPD modules are stacked and high energy photons hit the modules "edge-on". This provides "depth of interaction" (DOI) positioning, enabling 1 mm resolution in all three dimensions.

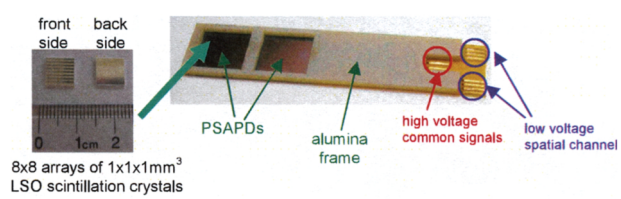

Fig. 2. Dual-LSO-PSAPD module. The flex circuit is seen in light-orange extending from under the edge of the white alumina cover used for mechanical support. Scintillation crystal arrays are placed on top of the PSAPD chips seen in dark brown through the window in the alumina.

Manuscript received November 14, 2008. This work was supported by NIH grants R01CA119056 and R33 EB003283. F.W.Y. Lau is supported by the Stanford Bio-X Graduate Student Fellowship. The authors thank Richard Farrell from RMD Inc. for useful discussions about the PSAPDs.

F.W.Y. Lau (email: flau@stanford.edu), P.D. Reynolds, F. Olutade, and M.A. Horowitz are in the Department of Electrical Engineering at Stanford University. C. Fang is in the Department of Mechanical Engineering and P. D. Olcott is in the Department of Bioengineering at Stanford. A. Vandenbroucke, V. C. Spanoudaki, and C. S. Levin (email: cslevin@stanford.edu) are in the Department of Radiology. All authors are associated with the Molecular Imaging Program at Stanford.

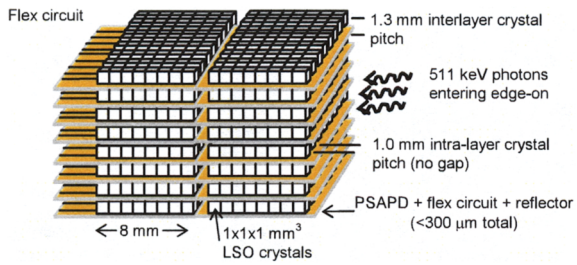

Fig. 3. Depiction of stack of Dual-LSO-PSAPD modules with directly measured 1 mm depth of interaction resolution.

C. Detector Characterization

Prototype detector modules were characterized using the RENA-3 data acquisition evaluation board (from NOVA R&D) and a 4 μCi Na-22 source. The results are shown in Fig. 4. The energy spectrum includes correction for per-crystal gain differences. Post-processing algorithms [2] corrected for amplitude walk and correlated noise to improve time resolution. All error bars are calculated using estimated statistical errors; systematic errors are ignored.

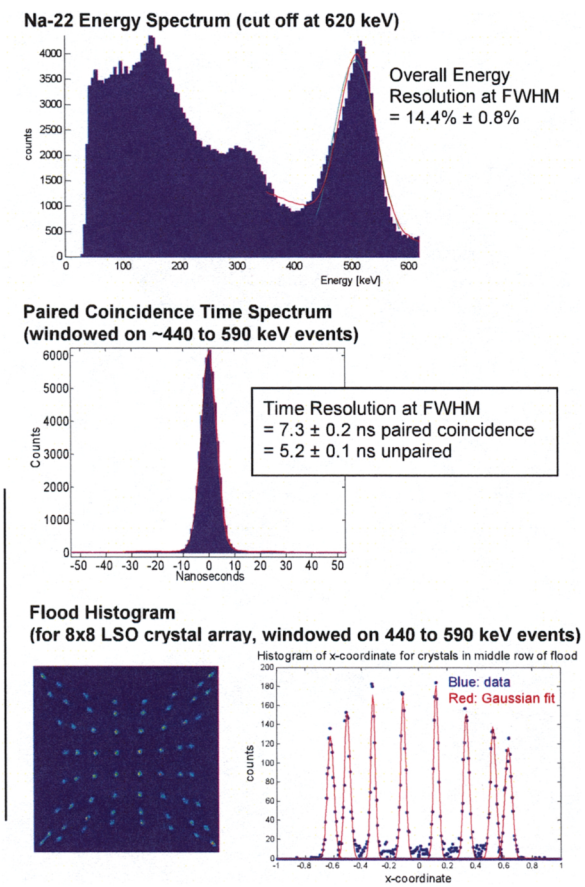

Fig. 4. Results from data acquisition using RENA-3 ASIC, with analog multiplexing [3] of two PSAPD's signals. Top: Energy spectrum. Middle: Paired coincidence time spectrum. Bottom: Flood histogram and profile of middle row of flood histogram showing a peak-to-valley ratio of about 14.

D. Sensor Card Assembly

Sixteen detector modules are arranged in a row, supported using an aluminum fin, to form a Sensor Card. Then these Sensor Cards are stacked, as shown in Fig 5.

Temperature regulation is needed since PSAPD performance is temperature dependent. There is no path for air flow between detector layers so we embed the detector modules in aluminum fins to draw the heat to the sides of the panel. At the sides, the heat is transferred and dissipated by the Peltier and water cooling. Studies on the effect of the aluminum fin on sensitivity and spatial resolution are in [4].

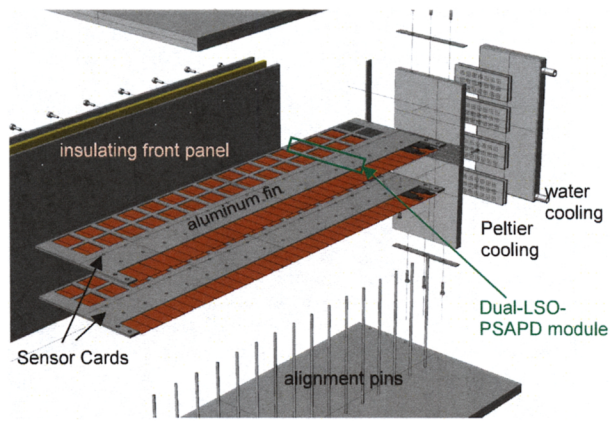

Fig. 5. Assembly of Sensor Cards and supporting and cooling structures.

E. Sensor Card Temperature Variation Simulation

A finite volume simulation of a Sensor Card was performed to analyze the temperature variation when only the edge is cooled, assuming the power dissipated by each PSAPD is 2.5 mW. Fig. 6 shows that the maximum temperature variation from the center to edge of a Sensor Card is only 4°C. We are currently studying how this 4°C variation in temperature degrades performance and if further thermal regulation efforts are needed.

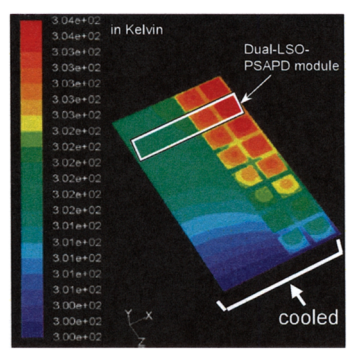

Fig. 6. Temperature variation across one-half of a Sensor Card in the detector panel stack (see Fig. 5), assuming the power dissipated by each PSAPD chip is 2.5 mW. Only half the Sensor Card was simulated due to symmetry.

F. Cartridge Assembly

A stack of eight Sensor Cards connected to data acquisition electronics forms a Cartridge. A cross-sectional view of a Cartridge is in Fig. 7. The Sensor Cards are soldered to intermediate flex circuits. An intermediate flex circuit is necessary to separate the high voltage signals (with DC component of -1750V) from the low voltage signals (with DC component of 0V) so we can use standard flex connectors to connect to the Discrete Board. The Discrete Board is a rigid printed circuit board (PCB) containing AC coupling, filtering, and attenuation circuitry. Details on the electronics on the Discrete Board are in [3].

The RENA Board contains arrays of RENA-3 chips, application specific integrated circuits (ASICs) developed by NOVA R&D (Irvine, CA). Each RENA-3 ASIC contains 36 channels of preamplifier, Gaussian shaper, trigger, sample-hold, and fast time stamp circuitry. Analog-to-digital converters (ADCs) on the RENA board immediately digitize the outputs of the RENA-3. Complex Programmable Logic Devices (CPLD) on the RENA Board program the RENA chips.

Field Programmable Gate Arrays (FPGAs) on the FPGA Board further process the RENA board outputs. The High Voltage (HV) Distribution Board provides programmable variable bias voltages for the PSAPDs.

G. HV Distribution Board Prototype

Since the optimal bias voltage for each PSAPD will differ depending on process and temperature variations, and it is not practical to manually adjust the bias voltage for each of the 4608 PSAPDs in the system, we needed a way to change the bias voltages using a computer so that in the future an algorithm can be used to calibrate the system. The HV Distribution Board provides this capability. We built a simplified prototype of the HV Distribution Board, shown in Fig. 8, which provides 64 channels of individually programmable high voltage.

The HV Distribution Board contains the Analog Devices AD5535 digital-to-analog (DAC) chip, which provides outputs with a 200V range. We operate this chip referenced to -1800V so that our board outputs range from -1800V to -1600V (relative to Earth Ground). All digital control signals from the computer interface with the AD5535 through optocouplers so there is >2000V isolation between the AD5535 circuit and Earth Ground.

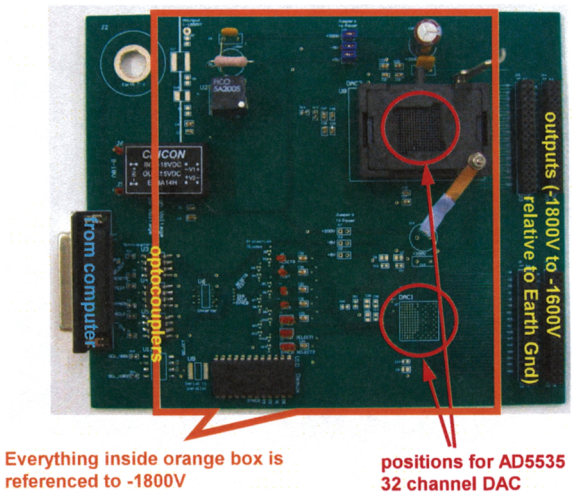

Fig. 8. High Voltage Distribution Board prototype allows application of varying biases to individual Dual LSO-PSAPD modules.

H. Imaging Head Assembly

As illustrated in Fig. 9, nine Cartridges are stacked to form an imaging head.

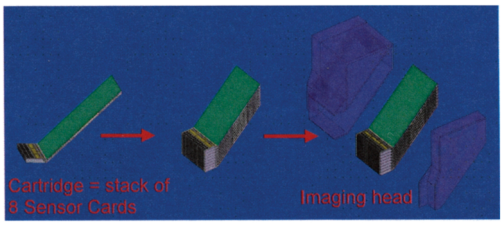

Fig. 9. Seven Cartridges are stacked to form an imaging head.

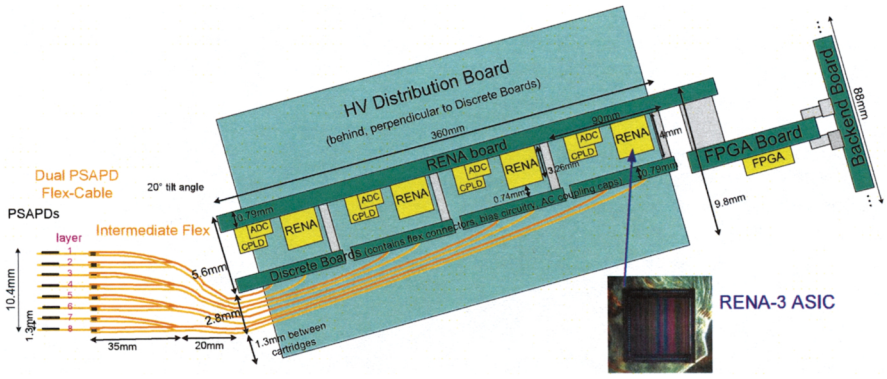

Fig. 7. Cartridge cross-sectional view, showing data acquisition chain.

Fig 10 shows a mechanical computer-aided-design (CAD) drawing of several Cartridges stacked together, showing the floor-plan of RENA Board electronics.

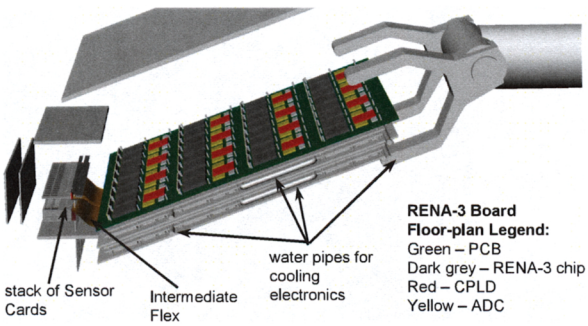

Fig. 10. Mechanical CAD drawing of several Cartridges stacked together, showing the floor-plan of RENA Board electronics as well as the structure to support each panel.

I. System Gantry

Since the system will be used in the operating room for guiding biopsy or cancer staging in addition to being used as an independent unit for diagnosis, it is important that the positioning of the imaging head be flexible so that we can use it under a biopsy bed. Therefore, the imaging head will be mounted on a mechanical arm, such as the one shown in Fig. 11, that provides six degrees of freedom so the head can be positioned anywhere in 3-dimensional space.

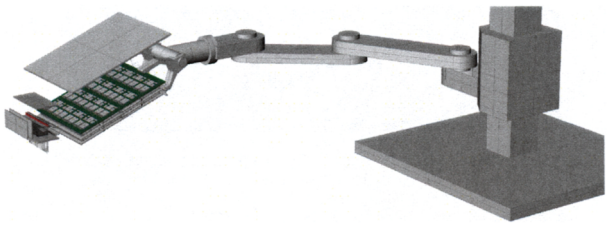

Fig. 11. System gantry, showing mechanical arm supporting the imaging heads.

J. List-mode, Pipelined Image Reconstruction

We will use list-mode 3D OSEM (ordered-subsets expectation-maximization) reconstruction to mitigate issues associated with incomplete angular sampling inherent to the dual-panel design and to achieve high resolution. Graphics Processor Units (GPUs) will accelerate the image reconstruction since reconstruction on a single GPU is >50x faster than on a single CPU [5]. List mode allows us to pipeline the image reconstruction while data is still being acquired.

III. Conclusions

The PET system under development will potentially increase the role of PET in breast cancer detection, diagnosis, biopsy, staging, and monitoring through its 1 mm^3 spatial resolution, 8 to 14% photon sensitivity, and portable system form factor. Work on scaling up the design from our prototype with a few modules to a full system with thousands of modules is underway.

References

[1] J. Zhang, P. D. Olcott, G. Chinn, A. M. K. Foudray, C.S. Levin, "Study of the Performance of a novel 1mm resolution dual-panel PET camera design dedicated to breast cancer imaging using Monte Carlo simulation," *Medical Physics*, vol. 34, no. 2, pp.689-702, Feb 2007.

[2] P. D. Reynolds, P. D. Olcott, G. Pratx, F. W. Y. Lau, C. S. Levin, "Convex Optimization of Coincidence Time Resolution for High Resolution PET systems," in *IEEE Nuclear Science Symposium and Medical Imaging Conference Record*, 2008.

[3] F. W. Y. Lau, A. Vandenbroucke, P. D. Reynolds, P. D. Olcott, M. A. Horowitz, C. S. Levin, "Front-end electronics for a $1mm^3$ resolution avalanche photodiode-based PET system with analog signal multiplexing," in *IEEE Nuclear Science Symposium and Medical Imaging Conference Record*, 2008.

[4] V. C. Spanoudaki, A. Vandenbroucke, F. W. Y. Lau, C. Fang, C. S. Levin, "Effects of Thermal Regulation Structures on the Photon Sensitivity and Spatial Resolution of a $1mm^3$ Resolution Breast-Dedicated PET System," in *Fourth International Workshop on the Molecular Radiology of Breast Cancer Conference Record*, 2008.

[5] G. Pratx, G. Chinn, P. D. Olcott, C. S. Levin. "Fast, Accurate and Shift-Varying Line Projections for Iterative Reconstruction Using the GPU," *IEEE Trans. Med. Imag.*, accepted for publication.